Supplemental Document: Interactive Hair Rendering and Appearance Editing under Environment Lighting

Kun Xu[1] Li-Qian Ma[1] Bo Ren[1] Rui Wang[2] Shi-Min Hu[1]

[1] TNList, Department of Computer Science and Technology, Tsinghua University, Beijing
[2] Department of Computer Science, University of Massachusetts, Amherst

This supplemental document provides additional proofs and results for the paper entitled *Interactive Hair Rendering and Appearance Editing under Environment Lighting*.

1 Approximating circular Gaussian by Gaussian

Using a 2nd-order Taylor expansion:

$$\cos(\phi-\mu) \approx 1-(\phi-\mu)^2/2$$

The circular Gaussian could be approximated by:

$$\begin{aligned} g^c(\phi;\mu,\lambda) &= \exp[\frac{2(\cos(x-\mu)-1)}{\lambda^2}] \\ &\approx \exp[-\frac{(\phi-\mu)^2}{\lambda^2}] = g(\phi;\mu,\lambda) \end{aligned}$$

This means a circular Gaussian can be well approximated by a Gaussian. When $\phi \in [\mu-\pi,\mu+\pi]$ and $\lambda < \pi/6$, the relative error of this approximation is $\leq 1.3\%$.

2 Product of two 1D Gaussians

A 1D Gaussian g is defined by $g(x;\mu,\lambda) = \exp(-(x-\mu)^2/\lambda^2)$ where μ is the center and λ is the width. Assume two 1D Gaussians $g_1(x;\mu_1,\lambda_1)$ and $g_2(x;\mu_2,\lambda_2)$, it is straightforward to prove that their product is still a Gaussian, given by $g_1 \cdot g_2 = b \cdot g_3(x;\mu_3,\lambda_3)$, where:

$$\begin{aligned} \mu_3 &= \frac{\mu_1/\lambda_1^2+\mu_2/\lambda_2^2}{1/\lambda_1^2+1/\lambda_2^2},\ \lambda_3 = \sqrt{\frac{1}{1/\lambda_1^2+1/\lambda_2^2}}, \\ b &= \exp\left(\frac{(\mu_1-\mu_2)^2}{\lambda_1^2+\lambda_2^2}\right). \end{aligned}$$

3 Product Integral of 1D Gaussians with Polynomials

First, the indefinite integral of a 1D Gaussian function $g(x;\mu,\lambda)$ is:

$$\int g(x;\mu,\lambda)\,dx = \frac{1}{2}\sqrt{\pi}\,\lambda\,\mathbf{erf}\left(\frac{x-\mu}{\lambda}\right)$$

where **erf** is the *error function* given by: $\mathbf{erf}(x) = \frac{2}{\sqrt{\pi}}\int_0^x e^{-t^2}dt$. It is also known that the indefinite product integral of a Gaussian function with the linear function x is computed as:

$$\int x\cdot g(x;\mu,\lambda)\,dx = -\frac{1}{2}\lambda^2 g(x;\mu,\lambda) + \frac{1}{2}\sqrt{\pi}\,\mu\,\lambda\,\mathbf{erf}\left(\frac{x-\mu}{\lambda}\right)$$

To evaluate the **erf** function, we can either use a precomputed table, or in our case, we use the following approximation [Abramowitz and Stegun 1964] that is easy to evaluate in a shader:

$$\mathbf{erf}(x) \approx 1-(a_1t+a_2t^2+a_3t^3)e^{-x^2},\quad t = 1/(1+px)$$

where $p = 0.47047$, $a_1 = 0.3480242$, $a_2 = -0.0958798$, $a_3 = 0.7478556$. This approximation is very accurate, and the approximation error is guaranteed to be smaller than 2.5×10^{-5}.

4 Integral of 1D circular Gaussian

The integral of a 1D circular Gaussian $g^c(\phi;\mu,\lambda)$ over $[-\pi,\pi]$ can be approximated as:

$$\int_{-\pi}^{\pi} g^c(\phi;\mu,\lambda)d\phi \approx \int_{-\pi}^{\pi} g(\phi;\mu,\lambda)d\phi \approx \int_{-\infty}^{\infty} g(\phi;\mu,\lambda)d\phi = \sqrt{\pi}\lambda$$

When $\lambda < \pi/6$, the relative error of this approximation is $\leq 1.9\%$.

5 Product of two 1D circular Gaussians

A circular Gaussian g^c is defined by $g^c(\phi;\mu,\lambda) = \exp[2(\cos(\phi-\mu)-1)/\lambda^2]$, which is a function of the angle ϕ on the circle. Assume two circular Gaussians $g_1^c(\phi;\mu_1,\lambda_1)$ and $g_2^c(\phi;\mu_2,\lambda_2)$, it is straightforward to prove that their product is still a circular Gaussian, given by $g_1^c \cdot g_2^c = b\cdot g_3^c(\phi;\mu_3,\lambda_3)$, where:

$$\begin{aligned} \mu_3 &= \arctan(n,m),\ \lambda_3 = \frac{1}{\sqrt[4]{m^2+n^2}}, \\ b &= \exp\left(-\frac{2}{\lambda_1^2}-\frac{2}{\lambda_2^2}+\frac{2}{\lambda_3^2}\right), \\ m &= \frac{\cos\mu_1}{\lambda_1^2}+\frac{\cos\mu_2}{\lambda_2^2},\ n = \frac{\sin\mu_1}{\lambda_1^2}+\frac{\sin\mu_2}{\lambda_2^2}. \end{aligned}$$

6 Definitions of $\overline{A}_b(\theta_d)$, $\overline{\Delta}_b(\theta_d)$, and $\overline{\sigma}_b(\theta_d)$ terms in Eq 29

According to [Zinke et al. 2008], these terms are all defined as functions of $\overline{a}_f(\theta_d)$, $\overline{a}_b(\theta_d)$, $\overline{\alpha}_f(\theta_d)$, $\overline{\alpha}_b(\theta_d)$, $\overline{\beta}_f(\theta_d)$, $\overline{\beta}_b(\theta_d)$, where $\overline{a},\overline{\alpha},\overline{\beta}$ stand for the average scattering attenuation, shift, and variance; and the subscripts f,b indicate the forward/backward scattering respectively. Specifically, their formulas are:

$$\begin{aligned} \overline{A}_b &= \frac{\overline{a}_b(\theta_d)\overline{a}_f^2(\theta_d)}{1-\overline{a}_f^2(\theta_d)} + \frac{\overline{a}_b^3(\theta_d)\overline{a}_f^2(\theta_d)}{(1-\overline{a}_f^2(\theta_d))^3} \\ \overline{\Delta}_b &\approx \overline{\alpha}_b\left(1-\frac{2\overline{a}_b^2}{(1-\overline{a}_f^2)^2}\right)+\overline{\alpha}_f\left(\frac{2(1-\overline{a}_f^2)^2+4\overline{a}_f^2\overline{a}_b^2}{(1-\overline{a}_f^2)^3}\right) \\ \overline{\sigma}_b &\approx (1+0.7\overline{a}_f^2)\frac{\overline{a}_b\sqrt{2\overline{\beta}_f^2+\overline{\beta}_b^2}+\overline{a}_b^3\sqrt{2\overline{\beta}_f^2+3\overline{\beta}_b^2}}{\overline{a}_b+\overline{a}_b^3(2\overline{\beta}_f+3\overline{\beta}_b)} \end{aligned}$$

where the average forward and backward scattering shifts $\overline{\alpha}_f,\overline{\alpha}_b$, and the average forward and backward scattering variances $\overline{\beta}_f^2,\overline{\beta}_b^2$

are calculated as (all sums are over $t \in \{R, TT, TRT\}$):

$$\overline{a}_f(\theta_d) = \sum_t \overline{a}_{f,t}(\theta_d) \quad , \quad \overline{a}_b(\theta_d) = \sum_t \overline{a}_{b,t}(\theta_d)$$

$$\overline{\alpha}_f(\theta_d) = \frac{\sum_t \overline{a}_{f,t}(\theta_d)\,\alpha_t}{\overline{a}_f(\theta_d)} \quad , \quad \overline{\alpha}_b(\theta_d) = \frac{\sum_t \overline{a}_{b,t}(\theta_d)\,\alpha_t}{\overline{a}_b(\theta_d)}$$

$$\overline{\beta}^2_f(\theta_d) = \frac{\sum_t \overline{a}_{f,t}(\theta_d)\,\beta_t^2}{\overline{a}_f(\theta_d)} \quad , \quad \overline{\beta}^2_b(\theta_d) = \frac{\sum_t \overline{a}_{b,t}(\theta_d)\,\beta_t^2}{\overline{a}_b(\theta_d)}$$

7 Proof of the integral of N_t in Eq 33

$$\int_{\frac{\pi}{2}}^{\frac{3\pi}{2}} \int_{-\frac{\pi}{2}}^{\frac{\pi}{2}} N_t(\theta_d, \phi_o - \phi_d)\, d\phi_d\, d\phi_o = 2\int_0^{\pi} \phi\, N_t(\theta_d, \phi) d\phi$$

The proof is given as follows:

$$\begin{aligned}
& \int_{\phi_o=\frac{\pi}{2}}^{\frac{3\pi}{2}} \int_{\phi_d=-\frac{\pi}{2}}^{\frac{\pi}{2}} N_t(\theta_d, \phi_o - \phi_d)\, d\phi_d\, d\phi_o \\
= & \int_{\phi_o=\frac{\pi}{2}}^{\frac{3\pi}{2}} \int_{\phi=\phi_o-\frac{\pi}{2}}^{\phi_o+\frac{\pi}{2}} N_t(\theta_d, \phi)\, d\phi\, d\phi_o \qquad (1) \\
= & \int_{\phi=0}^{2\pi} \int_{\phi_o=\max(\frac{\pi}{2}, \phi-\frac{\pi}{2})}^{\min(\frac{3\pi}{2}, \phi+\frac{\pi}{2})} N_t(\theta_d, \phi)\, d\phi_o\, d\phi \qquad (2) \\
= & \int_{\phi=0}^{2\pi} N_t(\theta_d, \phi)\, d\phi \int_{\max(\frac{\pi}{2}, \phi-\frac{\pi}{2})}^{\min(\frac{3\pi}{2}, \phi+\frac{\pi}{2})} d\phi_o \\
= & \; 2\int_{\phi=0}^{\pi} N_t(\theta_d, \phi)\, d\phi \int_{\max(\frac{\pi}{2}, \phi-\frac{\pi}{2})}^{\min(\frac{3\pi}{2}, \phi+\frac{\pi}{2})} d\phi_o \qquad (3) \\
= & \; 2\int_{\phi=0}^{\pi} N_t(\theta_d, \phi)\, d\phi \int_{\frac{\pi}{2}}^{\phi+\frac{\pi}{2}} d\phi_o \\
= & \; 2\int_{\phi=0}^{\pi} N_t(\theta_d, \phi)\, \phi\, d\phi
\end{aligned}$$

where step (1) uses the change of integral variable; step (2) switches the inner and outer intergrals; and step (3) is due to the symmetry of N_t with respect to ϕ.

8 Images of the precomputed 2D tables

In Fig 1, we show the images of all precomputed 2D tables used in this paper, including the 7 tables of $\mathscr{C}_k(\lambda'_j, \phi_o - \phi_j)$ $(0 \le k \le 6)$ for the R mode, 3 tables of $\mathscr{H}_k^{TT}(\eta, \theta_d)$ (k=0,2,4) for the TT mode, and 3 tables of $\mathscr{H}_k^{TRT}(\eta, \theta_d)$ (k=0,2,4) for the TRT mode. All of them are computed at a default resolution of 128×64. From the images we can see that these functions are smooth and hence our default resolution is sufficient.

9 Addition plots

In Fig 2 (next page) we show addition plots, including the single scattering inner integral $\mathscr{N}_t \cos^2\theta_i / \cos^2\theta_d$ computed for the three scattering modes, and the same for the global multiple scattering inner integral $\mathscr{N}_t^G \cos^2\theta_i / \cos^2\theta_d$. Note that these functions will be integrated with a 1D Gaussian using our linear quadrature method described in Section 4.2.2. By examining the smoothness of these functions in Fig 2 , we can see that our linear quadrature method is quite accurate in practice.

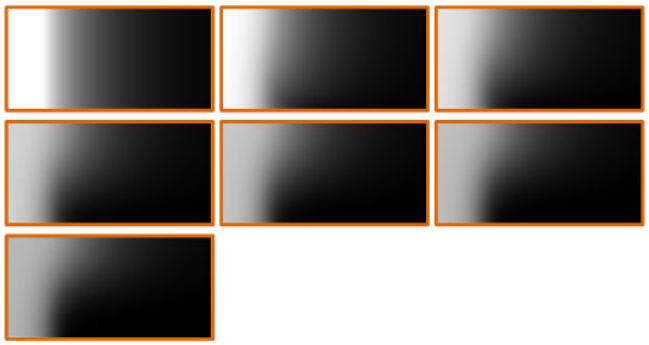

(a) The 7 tables of $\mathscr{C}_k(\lambda'_j, \phi_o - \phi_j)$ $(0 \le k \le 6)$ for the R mode.

(b) The 3 tables of $\mathscr{H}_k^{TT}(\eta, \theta_d)$ (k=0,2,4) for the TT mode

(c) The 3 tables of $\mathscr{H}_k^{TRT}(\eta, \theta_d)$ (k=0,2,4) for the TRT mode.

Figure 1: *Images of the precomputed 2D tables, all of which are computed at a resolution of* 128×64.

10 Addition Comparisons

In Fig 3, we compare the results of our method to [Ren et al. 2010] under a single SRBF light at different bandwidth λ. We observe that using SRBF ranging from small bandwidth ($\lambda = 0.01$) to large bandwidth ($\lambda = 0.8$), our method consistently matches [Ren et al. 2010] very well.

In Fig 4, we provide a comparison between renderings computed with directional lights vs. SRBF lights. We observe that using only 10 SRBFs already leads to more accurate result than using 240 directional lights. This is because the environment map used for this example – Eucalyptus Grove – has a wide region of sky light, which requires a large number of directional lights to approximate well.

References

ABRAMOWITZ, M., AND STEGUN, I. A. 1964. *Handbook of Mathematical Functions with Formulas, Graphs, and Mathematical Tables*. Dover, New York.

ZINKE, A., YUKSEL, C., WEBER, A., AND KEYSER, J. 2008. Dual scattering approximation for fast multiple scattering in hair. *ACM Trans. Graph. 27*, 3, 32:1–32:10.

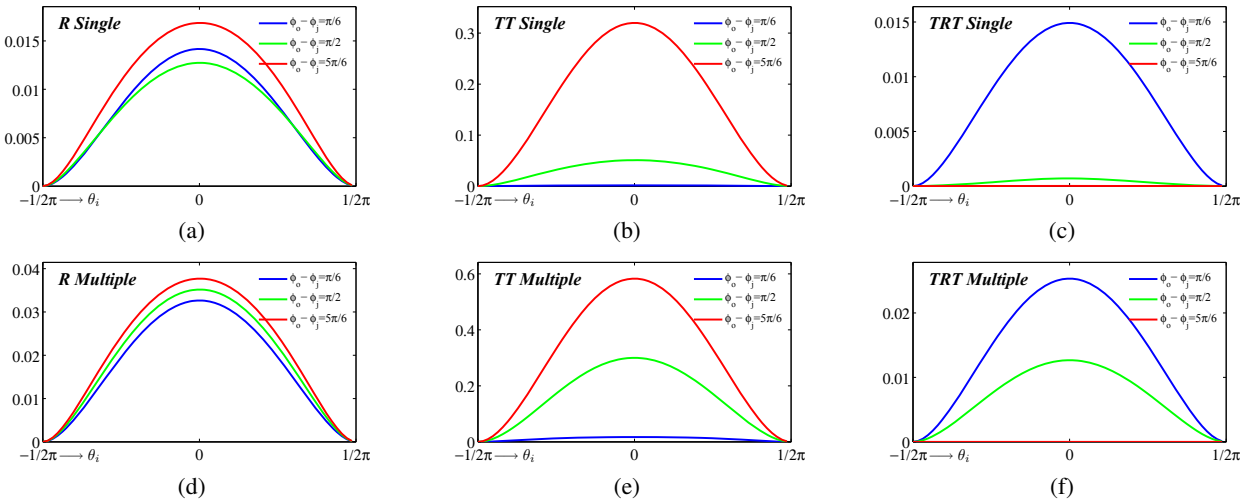

Figure 2: *The top three figures show $\mathcal{N}_t \cos^2\theta_i / \cos^2\theta_d$ (in single scattering) computed for the three scattering modes. The bottom three figures show the same for $\mathcal{N}_t{}^G \cos^2\theta_i / \cos^2\theta_d$ (in multiple scattering). Note that all these functions are very smooth.*

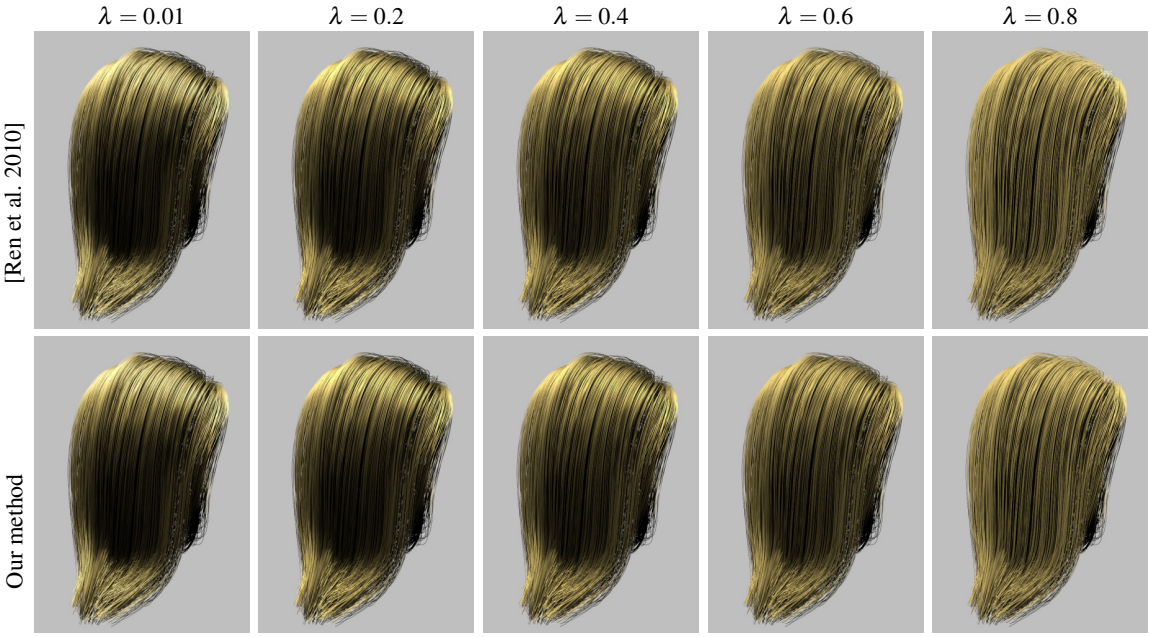

Figure 3: *Comparison of our method (bottom row) to [Ren et al. 2010] (top row) under a single SRBF light at different bandwidth λ. Note from small SRBF bandwidth ($\lambda = 0.01$) to large bandwidth ($\lambda = 0.8$), our method consistently matches [Ren et al. 2010] well.*

(a) 10 DLs (b) 240 DLs (c) 10 SRBFs (d) 30 SRBFs (e) reference

Figure 4: *Comparison of results using directional lights (DL) and SRBF lights. In (a) and (b), the environment map is approximated as 10 and 240 directional lights (i.e. zero support size), respectively; (c) and (d) show our result by approximating the environment map as 10 and 30 SRBF lights, respectively. (e) is the reference image. Note that using only 10 SRBFs already leads to more accurate result than using 240 directional lights.*